Arch Appl Mech (2014) 84:95–107
DOI 10.1007/s00419-013-0785-y

ORIGINAL

A. A. Hejazi · M. Ayatollahi · R. Bagheri · M. M. Monfared

Dislocation technique to obtain the dynamic stress intensity factors for multiple cracks in a half-plane under impact load

Received: 15 December 2012 / Accepted: 5 September 2013 / Published online: 29 September 2013

Abstract In this study, the transient response of multiple cracks subjected to shear impact load in a half-plane is investigated. At first, exact analytical solution for the transient response of Volterra-type dislocation in a half-plane is obtained by using the Cagniard-de Hoop method of Laplace inversion and is expressed in explicit forms. The distributed dislocation technique is used to construct integral equations for a half-plane weakened by multiple arbitrary cracks. These equations are of Cauchy singular type at the location of dislocation solved numerically to obtain the dislocation density on the cracks faces. The dislocation densities are employed to determine dynamic stress intensity factors history for multiple smooth cracks. Finally, several examples are presented to demonstrate the applicability of the proposed solution.

Keywords Half-plane · Transient · Volterra dislocation · Curved crack · Dynamic stress intensity factors

1 Introduction

In recent years, due to the growing demands for predicting the behavior of cracked structures during impact and crash events, the importance of fracture mechanics has increased considerably in engineering applications. In the fracture mechanics of materials, great efforts have been made to study the static fracture behavior of materials. Most of the studies, however, are related to static or quasi-static conditions. But it may be very important to study the response of cracks under dynamic loading. This is because of the mathematical complications. In the case of dynamic loads, two loading cases are of interest. Harmonic loading and impact loading. The dynamic stress intensity factor plays an important role in dynamic fracture under both harmonic and impacts loads, which predicts whether or not the fracture toughness of the material will be exceeded and catastrophic crack propagation will follow. Apparently, the first study dealing with dynamic crack problems was conducted by Maue [1]. He analyzed a semi-infinite crack in an infinite plane under time-harmonic stress wave by means of the Wiener-Hopf technique. The dynamic stress intensity factor for a finite crack in the infinite plane under anti-plane deformation was determined by Loeber and Sih [2]. Thau and Hwei obtained the transient stress intensity factors for a finite crack exposed to a longitudinal shock wave [3]. Dynamic stress intensity factors have been given for a penny-shaped circular crack subjected to an impact load by Sih and Embley [4]. The transient response of finite cracks in orthotropic materials has been presented by Kuo [5]. The dynamic stress intensity factors have been derived by Ang [6] for a crack in a layered transversely isotropic material under action of impact loading. Babaei and Lukasiewicz [7] considered a transient dynamic problem of a crack in a non-homogeneous layer between two dissimilar elastic half-planes. The dynamic stress intensity

A. A. Hejazi · M. Ayatollahi (✉) · R. Bagheri · M. M. Monfared
Faculty of Engineering, University of Zanjan, P.O. Box 45195-313, Zanjan, Iran
E-mail: mo_ayatollahy@yahoo.com

R. Bagheri
E-mail: rasul_m65@yahoo.com

factor for mode III loading has been solved by Wang et al. [8]; they analyzed the anti-plane response of a non-homogeneous composite material containing several cracks subjected to dynamic impact. The transient response of a finite crack in an infinite piezoelectric medium due to electromechanical loads was investigated by Chen and Karihaloo [9]. Zhang [10] investigated the transient analysis of a crack in anisotropic solid. Results show the effect of material anisotropy on the dynamic stress intensity factors. The transient dynamic stress intensity factor was determined for an interface crack between two dissimilar half-infinite isotropic viscoelastic bodies under impact loading by Wei et al. [11]. Zhao et al. [12], was studied the dynamic behavior of a bonded piezoelectric and elastic half-space containing multiple interfacial collinear cracks subjected to transient electro-mechanical loads. A transient dynamic crack analysis for a functionally graded material has been presented by Zhang et al. [13]. They analyzed dynamic overshoot over the corresponding static stress intensity factors. The mode I extension of a half-plane crack in a transversely isotropic solid under 3-D loading was analyzed by Zhao [14]. Feng and Zou [15] considered torsion impact response of penny-shaped crack in a transversely isotropic strip. Results show the effects of material non-homogeneity, orthotropy, and thickness of strip on the dynamic stress intensity factor. Sladek et al. [16] used both the meshless method and the Stehfest inversion algorithm to simulate the dynamic response of FGMs under anti-plane shear impact load. A periodic array of cracks in an infinite functionally graded material under transient mechanical loading was investigated by Wang and Mai [17]. Itou [18] investigated the transient dynamic stress intensity factors around two rectangular cracks in a non-homogeneous interfacial layers sandwiched between two dissimilar elastic half-spaces. The problem of a homogeneous linear elastic body containing multiple collinear cracks under anti-plane dynamic load was considered by Wu and Chen [19]. In spite of these efforts, all of the above-mentioned references are concerned with the dynamic behavior of a medium containing straight cracks with simple patterns. The solution procedures devised in all the above studies are neither capable of handling curved cracks among multiple cracks with arbitrary arrangement. Monfared and Ayatollahi [20] investigated the elastodynamic analysis of multiple cracks in an orthotropic half-plane under time-harmonic anti-plane loading. Results show the effect of material and geometric parameters upon the dynamic stress intensity factor.

In this article, the distributed dislocation technique is employed to derive singular integral equations for multiple cracks in the half-plane under impact loading. The solution of dislocations problem is carried out by utilizing Cagniard-de Hoop method with the aid of one-sided and two-sided Laplace transforms. One-sided and two-sided Laplace transforms in conjunction with Cagniard-de Hoop method prove to be powerful tools in obtaining analytical solutions. The dislocation solutions are then used to formulate integral equations for a half-plane weakened by several cracks. The integral equations are of Cauchy singular types which are solved numerically for the dislocation density on the cracks faces. Finally, numerical calculations have been carried out to show the influences of geometric parameters and crack configuration upon the dynamic stress intensity factor of cracks.

2 Description of the problem

The problem under consideration is described in Fig. 1. A half-plane contains Volterra-type dislocation. The system of rectangular Cartesian coordinates is introduced in the half-plane in such a way that the dislocation line is $y = 0, x \geq 0$. The distance between the x-axis and the half-plane boundary is h; therefore, $0 \leq y \leq h$

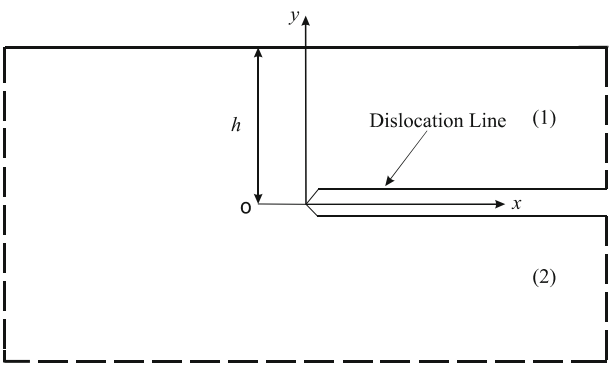

Fig. 1 Half-plane weakened by Volterra dislocation

and $y \leq 0$. For a medium under anti-plane deformation, the only nonzero displacement component is the out of plane component $w(x, y, t)$. Under the anti-plane shear load, the strain deformation can be described by

$$\gamma_{zx} = \frac{\partial w}{\partial x}, \gamma_{zy} = \frac{\partial w}{\partial y}. \tag{1}$$

Substituting Eq. (1) into Hook's law leads to the stress components in terms of displacement field

$$\begin{aligned} \sigma_{zx}(x, y, t) &= \mu \frac{\partial w}{\partial x}, \\ \sigma_{zy}(x, y, t) &= \mu \frac{\partial w}{\partial y}. \end{aligned} \tag{2}$$

In the above equation, μ is an elastic modulus of material. The basic equation which governs the anti-plane deformation behavior of the half-plane called equation of motion. That can be expressed in the form

$$\frac{\partial^2 w}{\partial x^2} + \frac{\partial^2 w}{\partial y^2} = S_L^2 \frac{\partial^2 w}{\partial t^2}. \tag{3}$$

where S_L^2 is wave slownesses defined by $S_L = 1/c_L$ and $c_L = \sqrt{\mu/\rho}$ being the shear wave speed, ρ is the mass density of half-plane. We consider a Volterra dislocation with Burgers vectors b_z located at the origin. To facilitate the solution of Eq. (3), the dislocation line is chosen to be the positive part of the x-axis. Therefore, the dislocation and boundary conditions are:

$$\begin{aligned} &w(x, 0^+, t) - w(x, 0^-, t) = b_z H(x) H(t), \\ &\sigma_{zy}(x, 0^+, t) = \sigma_{zy}(x, 0^-, t), \\ &\lim_{y \to -\infty} \sigma_{zy}(x, y, t) = 0, \\ &\lim_{|x| \to \infty} w(x, y, t) = 0, \\ &\sigma_{zy}(x, h) = 0. \end{aligned} \tag{4}$$

The unit step function $H(\ldots)$ is the Heaviside unit-function. It is worth mentioning that the above conditions for Volterra dislocation were utilized by several investigators, e.g., Weertman [21]. Since the medium is initially undisturbed, initial conditions take the following forms

$$\begin{aligned} \dot{w}(x, y, 0) &= 0, \\ w(x, y, 0) &= 0. \end{aligned} \tag{5}$$

3 Method of solution

The solution to Eq. (3) is accomplished by means of the two-sided Laplace transformations defined as

$$f^*(\zeta) = \int_{-\infty}^{+\infty} f(x) e^{-\zeta x} \mathrm{d}x. \tag{6}$$

The inversion of (6) is

$$f(x) = \frac{1}{2\pi i} \int_{\zeta_1 - \infty}^{\zeta_1 + \infty} f^*(\zeta) e^{\zeta x} \mathrm{d}\zeta. \tag{7}$$

Define one-sided Laplace pair by

$$f(t) = \frac{1}{2\pi i}\int_{Br} \bar{f}(s)\exp(st)\mathrm{d}s,$$
$$\bar{f}(s) = \int_{0}^{+\infty} f(t)\exp(-st)\mathrm{d}t, \tag{8}$$

where Br denotes the Bromwich path in pertinent complex plane and the Laplace transform parameters is taken as positive number. The general solution of the Eq. (3) is obtained by applying the one-sided Laplace transform over time and two-sided Laplace transform over the spatial coordinate x. Upon application of the above-mentioned integral transform with the aid of bounded condition $\lim_{|x|\to\infty} w(x, y, t) = 0$, Eq. (3) reduce to the ordinary differential equation for $w^*(\zeta, y, s)$ which can be readily solved. The bounded solution to this equation under the condition $Re[(S_L s)^2 - \zeta^2] \geq 0$ where Re designates the real part of the expression yields:

$$\bar{w}_1^*(\zeta, y, s) = A_1(\zeta, s)e^{-y\sqrt{S_L^2 s^2-\zeta^2}} + B_1(\zeta, s)e^{y\sqrt{S_L^2 s^2-\zeta^2}} \qquad 0 \leq y \leq h,$$
$$\bar{w}_2^*(\zeta, y, s) = B_2(\zeta, s)e^{y\sqrt{S_L^2 s^2-\zeta^2}} \qquad y \leq 0. \tag{9}$$

where $A_1(\zeta, s)$, $B_1(\zeta, s) and B_2(\zeta, s)$ are the unknown coefficients that will be obtained by applying Fourier and Laplace transformation to Eq. (4) with initial condition (5), and using Eq. (9), the result obtained is

$$\begin{bmatrix} A_1 \\ B_1 \\ B_2 \end{bmatrix} = \frac{b_z}{2\zeta s}\begin{bmatrix} 1 \\ e^{-2h\sqrt{S_L^2 s^2-\zeta^2}} \\ e^{-2h\sqrt{S_L^2 s^2-\zeta^2}-1} \end{bmatrix}. \tag{10}$$

Substituting (10) into (9) yields the displacement field in the half-plane

$$\bar{w}_1^*(\zeta, y, s) = \frac{b_z}{2\zeta s}\left[e^{-y\sqrt{S_L^2 s^2-\zeta^2}} + e^{(y-2h)\sqrt{S_L^2 s^2-\zeta^2}}\right],$$
$$\bar{w}_2^*(\zeta, y, s) = \frac{b_z}{2\zeta s}\left[e^{(y-2h)\sqrt{S_L^2 s^2-\zeta^2}} - e^{y\sqrt{S_L^2 s^2-\zeta^2}}\right]. \tag{11}$$

By applying (7) to (11), we obtain

$$\bar{w}_1(x, y, s) = -\frac{ib_z}{4\pi s}\int_{-\infty}^{+\infty} \frac{\left(e^{-y\sqrt{S_L^2 s^2-\zeta^2}} + e^{(y-2h)\sqrt{S_L^2 s^2-\zeta^2}}\right)e^{\zeta x}}{\zeta}\mathrm{d}\zeta \qquad 0 \leq y \leq h,$$
$$\bar{w}_2(x, y, s) = -\frac{ib_z}{4\pi s}\int_{-\infty}^{+\infty} \frac{\left(e^{(y-2h)\sqrt{S_L^2 s^2-\zeta^2}} - e^{y\sqrt{S_L^2 s^2-\zeta^2}}\right)e^{\zeta x}}{\zeta}\mathrm{d}\zeta \qquad y \leq 0. \tag{12}$$

Let us introduce the following substitution in the expression for $\bar{w}(x, y, p)$, Eq. (12), $\zeta = s\eta$, where s, which is the variable of the one-sided Laplace transform, is assumed real and positive. The final result can be written as:

$$\bar{w}_1(x, y, s) = -\frac{ib_z}{4\pi s}\int_{-\infty}^{+\infty} \frac{\left(e^{-ys\sqrt{S_L^2-\eta^2}} + e^{(y-2h)s\sqrt{S_L^2-\eta^2}}\right)e^{s\eta x}}{\eta}\mathrm{d}\eta \qquad 0 \leq y \leq h,$$
$$\bar{w}_2(x, y, s) = -\frac{ib_z}{4\pi s}\int_{-\infty}^{+\infty} \frac{\left(e^{(y-2h)s\sqrt{S_L^2-\eta^2}} - e^{ys\sqrt{S_L^2-\eta^2}}\right)e^{s\eta x}}{\eta}\mathrm{d}\eta \qquad y \leq 0. \tag{13}$$

The integrand in Eq. (13) is a multi-valued function with branch points at $\eta = \pm S_L$. The idea of the Cagniard-de Hoop method is to deform the path of integration in the η-plane. To carry out the integration in (13), the procedure outlined in Achenbach [22] is followed. The details of manipulation are given in Appendix. For the sake of brevity, the details of manipulation are not given here. The final result is

$$w(x,y,t) = \frac{b_z}{2\pi}\left[\tan^{-1}\left(\frac{x\sqrt{(t-S_Lr_1)/(t+S_Lr_1)}}{r_1+y}\right) - \tan^{-1}\left(\frac{x\sqrt{(t-S_Lr_1)/(t+S_Lr_1)}}{r_1-y}\right)\right]H(t-S_Lr_1)$$
$$+\frac{b_z}{2\pi}\left[\tan^{-1}\left(\frac{x\sqrt{(t-S_Lr_2)/(t+S_Lr_2)}}{r_2+(2h-y)}\right) - \tan^{-1}\left(\frac{x\sqrt{(t-S_Lr_2)/(t+S_Lr_2)}}{r_2-(2h-y)}\right)\right]H(t-S_Lr_2). \tag{14}$$

The corresponding anti-plane shear stress distributions in Laplace transform may be obtained by substituting Eq. (13) into the Eq. (1) and carrying out some elementary manipulation. The final solution yields:

$$\bar{\sigma}_{1zx}(x,y,s) = -\frac{i\mu b_z}{4\pi}\int_{-\infty}^{\infty}\left(e^{-ys\sqrt{S_L^2-\eta^2}} + e^{(y-2h)s\sqrt{S_L^2-\eta^2}}\right)e^{s\eta x}\,\mathrm{d}\eta,$$

$$\bar{\sigma}_{2zx}(x,y,s) = -\frac{i\mu b_z}{4\pi}\int_{-\infty}^{\infty}\left(e^{(y-2h)s\sqrt{S_L^2-\eta^2}} - e^{ys\sqrt{S_L^2-\eta^2}}\right)e^{s\eta x}\,\mathrm{d}\eta, \qquad 0 \le y \le h$$

$$\bar{\sigma}_{1zy}(x,y,s) = -\frac{i\mu b_z}{4\pi}\int_{-\infty}^{\infty}\frac{\sqrt{S_L^2-\eta^2}\left(e^{(y-2h)s\sqrt{S_L^2-\eta^2}} - e^{-ys\sqrt{S_L^2-\eta^2}}\right)e^{s\eta x}}{\eta}\,\mathrm{d}\eta,$$

$$\bar{\sigma}_{2zy}(x,y,s) = -\frac{i\mu b_z}{4\pi}\int_{-\infty}^{\infty}\frac{\sqrt{S_L^2-\eta^2}\left(e^{(y-2h)s\sqrt{S_L^2-\eta^2}} - e^{ys\sqrt{S_L^2-\eta^2}}\right)e^{s\eta x}}{\eta}\,\mathrm{d}\eta. \qquad y \le 0 \tag{15}$$

A procedure identical to that employed for carrying out the integration in Eq. (15). For the sake of brevity, the details of manipulation are not given here. The final results are:

$$\sigma_{zx}(x,y,t) = \frac{\mu b_z t}{2\pi}\left[\frac{y}{r_1^2\sqrt{t^2-S_L^2r_1^2}}H\left(t-S_L^2r_1\right) - \frac{(y-2h)}{r_2^2\sqrt{t^2-S_L^2r_2^2}}H\left(t-S_L^2r_2\right)\right],$$

$$\sigma_{zy}(x,y,t) = -\frac{\mu b_z xt}{2\pi}\left[\frac{1}{\sqrt{t^2-S_L^2r_1^2}}\left(\frac{1}{r_1^2} - \frac{S_L^2}{t^2-S_L^2y^2}\right)H\left(t-S_L^2r_1\right)\right.$$
$$\left. -\frac{1}{\sqrt{t^2-S_L^2r_2^2}}\left(\frac{1}{r_2^2} - \frac{s_l^2}{t^2-S_L^2(y-2h)^2}\right)H\left(t-S_L^2r_2\right)\right]. \tag{16}$$

We observe that stress components are Cauchy singular at the dislocation position which is a well-known feature of stress fields due to Volterra dislocation. Let the half-plane, in the absence of cracks, be subjected to a shear impact point force of magnitude τ_0 represented by

$$\sigma_{zy}(x,h,t) = \tau_0\delta(x)H(t) \tag{17}$$

where $\delta(x)$ and $H(t)$ are the Dirac delta function and Heaviside step function, respectively. Equation (3) should be solved subjected to the above boundary condition. The problem is symmetric with respect to the y-axis. With the aid of one-sided and two-sided Laplace transform to Eq. (3) and following the procedure similar to that for dislocation solution leads to displacement field as

$$\bar{w}(x,y,s) = \frac{\tau_0}{2\pi is\mu}\int_{-\infty}^{+\infty}\frac{\left(e^{-(h-y)\sqrt{S_L^2s^2-\zeta^2}+\zeta x}\right)}{\sqrt{S_L^2s^2-\zeta^2}}\,\mathrm{d}\zeta \tag{18}$$

Utilizing Eqs. (3) and (18), the stress components become:

$$\sigma_{zx}(x, y, t) = \frac{\tau_0 x t}{\pi r^2 \sqrt{t^2 - S_L^2 r^2}} H(t - S_L r),$$
$$\sigma_{zy}(x, y, t) = \frac{\tau_0 (h - y) t}{\pi r^2 \sqrt{t^2 - S_L^2 r^2}} H(t - S_L r). \tag{19}$$

We observe that stress components are Cauchy singular at the point of application of load.

4 Analyses with multiple cracks

The dislocation solution accomplished in the foregoing section is extended to analyze half-plane with several cracks. Let Volterra dislocation with density b_z is distributed on a curved crack with parametric equations, $x = \alpha(p)$, $y = \gamma(p) - 1 \le p \le 1$ in the half-plane, that it should satisfy smoothness requirements. By virtue of Eq. (16), the stress fields caused at a point by the above-mentioned distribution of dislocation become:

$$\sigma_{zx}(x, y, t) = \frac{\mu t}{2\pi} \int_{-1}^{1} \sqrt{[\alpha'(p)]^2 + [\gamma'(p)]^2} \left[\frac{(y - \gamma) H(t - S_L r_1)}{r_1^2 \sqrt{t^2 - S_L^2 r_1^2}} + \frac{(2h - (y - \gamma)) H(t - S_L r_2)}{r_2^2 \sqrt{t^2 - S_L^2 r_2^2}} \right] b_z(p) \mathrm{d}p$$
$$\sigma_{zy}(x, y, t) = -\frac{\mu t}{2\pi} \int_{-1}^{1} \sqrt{[\alpha'(p)]^2 + [\gamma'(p)]^2} \left[\frac{(x - \alpha) H(t - S_L r_1)}{\sqrt{t^2 - S_L^2 r_1^2}} \left(\frac{1}{r_1^2} - \frac{S_L^2}{t^2 - S_L^2 (y - \gamma)^2} \right) - \frac{(x - \alpha) H(t - S_L r_2)}{\sqrt{t^2 - S_L^2 r_2^2}} \left(\frac{1}{r_2^2} - \frac{s_l^2}{t^2 - S_L^2 ((y - \gamma) - 2h)^2} \right) \right] b_z(p) \mathrm{d}p \tag{20}$$

In Eq. (20), $r_1 = \sqrt{(x - \alpha(p))^2 + (y - \gamma(p))^2}$, $r_2 = \sqrt{(x - \alpha(p))^2 + ((y - \gamma(p)) - 2h)^2}$, and prime denotes differentiation with respect to the relevant argument. The moveable orthogonal t, n-coordinate system is chosen such that the origin may move on the crack while t-axis remains tangent to the crack surface. The anti-plane stress components on the local coordinate, located on the surface of the i-th crack, become:

$$\sigma_{nz}(x_i, y_i, t) = \sigma_{zy} \cos\theta_i(s) - \sigma_{zx} \sin\theta_i(s), i \in \{1, 2, \ldots, N\} \tag{21}$$

where $\theta_i(s) = \tan^{-1}(\gamma_i'(s)/\alpha_i'(s))$ is the angle between x-and s-axes on the ith crack. A crack is constructed by continuous distribution of dislocations; therefore, the traction on the face of ith crack due to the presence of above-mentioned distribution of dislocations on the face of all N cracks yields:

$$\sigma_{nz}(\alpha_i(s), \gamma_i(s), t) = \sum_{j=1}^{N} \int_{-1}^{1} K_{ij}(s, p, t) \sqrt{[\alpha_i'(s)]^2 + [\gamma_i'(s)]^2} B_{zj}(p) \mathrm{d}p \quad i = 1, 2, \ldots, N \tag{22}$$

From Eqs. (20) and (21), the kernel of integral (22) becomes:

$$K_{ij}(\alpha_i(s), \gamma_i(s), \alpha_j(p), \gamma_j(p), t) = -\frac{t\mu}{2\pi} \left\{ (\alpha_i - \alpha_j) \left[\frac{1}{\sqrt{t^2 - S_L^2 r_{ij1}^2}} \left(\frac{1}{r_{ij1}^2} - \frac{S_L^2}{t^2 - S_L^2 (\gamma_i - \gamma_j)^2} \right) H\left(t - S_L r_{ij1}\right) - \frac{1}{\sqrt{t^2 - S_L^2 r_{ij2}^2}} \left(\frac{1}{r_{ij2}^2} - \frac{S_L^2}{t^2 - S_L^2 ((\gamma_i - \gamma_j) - 2h)^2} \right) H\left(t - S_L r_{ij2}\right) \right] \cos\theta_i(s) + \left[\frac{(\gamma_i - \gamma_j) H(t - S_L r_{ij1})}{r_{ij1}^2 \sqrt{t^2 - S_L^2 r_{ij1}^2}} + \frac{(2h - (\gamma_i - \gamma_j)) H(t - S_L r_{ij2})}{r_{ij2}^2 \sqrt{t^2 - S_L^2 r_{ij2}^2}} \right] \sin\theta_i(s) \right\} \tag{23}$$

where $r_{ij1} = \sqrt{(\alpha_i - \alpha_j)^2 + (\gamma_i - \gamma_j)^2}$ and $r_{ij2} = \sqrt{(\alpha_i - \alpha_j)^2 + ((\gamma_i - \gamma_j) - 2h)^2}$. The elasticity problem of a half-plane in the absence of cracks under impact concentrated load is solved in the previous section and the stress components are determined. By virtue of the Buckner's principal, the stress components with opposite sign should be substituted in Eq. (22) to determine the traction on a crack face which is the left-hand side of Eq. (22). From (21) and (22), we obtain the following singular integral equations:

$$\sum_{j=1}^{N} \int_{-1}^{1} t \left\{ (\alpha_i - \alpha_j) \left[\frac{1}{\sqrt{t^2 - S_L^2 r_{ij1}^2}} \left(\frac{1}{r_{ij1}^2} - \frac{S_L^2}{t^2 - S_L^2(\gamma_i - \gamma_j)^2} \right) H(t - S_L r_{ij1}) \right. \right.$$
$$\left. + \frac{1}{\sqrt{t^2 - S_L^2 r_{ij2}^2}} \left(\frac{1}{r_{ij2}^2} - \frac{S_L^2}{t^2 - S_L^2((\gamma_i - \gamma_j) - 2h)^2} \right) H(t - S_L r_{ij2}) \right] \cos\theta_i(s)$$
$$\left. + \left[\frac{(\gamma_i - \gamma_j) H(t - S_L r_{ij1})}{r_{ij1}^2 \sqrt{t^2 - S_L^2 r_{ij1}^2}} + \frac{(2h - (\gamma_i - \gamma_j)) H(t - S_L r_{ij2})}{r_{ij2}^2 \sqrt{t^2 - S_L^2 r_{ij2}^2}} \right] \sin\theta_i(s) \right\} \sqrt{[\alpha_i'(s)]^2 + [\gamma_i'(s)]^2} B_{zj}(p) \mathrm{d}p$$
$$= -\frac{2\pi \sigma_{nz}(\alpha_i(s), \gamma_i(s), t)}{\mu}, i = 1, 2, \ldots, N. \quad t > 0 \tag{24}$$

It is worth mentioning that kernels in integral Eq. (24) are Cauchy singular. Employing the definition of dislocation density function, the equations for the crack opening displacement across the jth crack become:

$$w_j^-(s) - w_j^+(s) = \int_{-1}^{s} \sqrt{(\alpha_i'(p))^2 + (\gamma_i'(p))^2} B_{zj}(p) \mathrm{d}p, \; j = 1, 2, \ldots, N. \tag{25}$$

Let the half-plane weakened by N_1 and N_2 be embedded and edge cracks, respectively. The displacement field away from the surfaces of embedded cracks is single-valued. Consequently, the dislocation density functions are subject to the following closure requirements

$$\int_{-1}^{1} \sqrt{(\alpha_i'(p))^2 + (\gamma_i'(p))^2} B_{zj}(p) \mathrm{d}p = 0, \; j = 1, 2, \ldots, N_1. \tag{26}$$

5 Solution of the singular integral equations

To obtain the dislocation density for embedded cracks, the integral equations (22) and (26) are to be solved simultaneously. This task is taken up by means of Gauss–Chebyshev quadrature scheme developed in [23]. Stress fields for the embedded cracks in isotropic materials are singular at crack tips with square-root singularity. Hence, the dislocation density functions for embedded cracks can be represented by

$$B_{zj}(p) = \frac{g_{zj}(p)}{\sqrt{1 - p^2}}, -1 \le p \le 1, \; j = 1, 2, \ldots, N_1. \tag{27}$$

For the edge cracks, taking the embedded crack tip at $p = -1$, the following dislocation density function is considered:

$$B_{zj}(p) = g_{zj}(p) \sqrt{\frac{1 - p}{1 + p}}, -1 \le p \le 1, \; j = N_1 + 1, \ldots, N. \tag{28}$$

The functions $g_{zj}(p)$ in above equation are continuous in $-1 \le p \le 1$. It is known that the stress intensity factors for a given crack in terms of the crack opening displacement are given by [24].

$$k_{Li} = \frac{\sqrt{2}}{4} \mu \lim_{r_{Li} \to 0} \frac{w_j^+(s) - w_j^-(s)}{\sqrt{r_{Li}}},$$
$$k_{Ri} = \frac{\sqrt{2}}{4} \mu \lim_{r_{Ri} \to 0} \frac{w_j^+(s) - w_j^-(s)}{\sqrt{r_{Ri}}}. \tag{29}$$

where L and R designate the left and right tips of a crack, respectively. The geometry of a crack implies:

$$r_{Li} = \left[(\alpha_i(s) - \alpha_i(-1))^2 + (\gamma_i(s) - \gamma_i(-1))^2\right]^{\frac{1}{2}},$$
$$r_{Ri} = \left[(\alpha_i(s) - \alpha_i(1))^2 + (\gamma_i(s) - \gamma_i(1))^2\right]^{\frac{1}{2}}. \tag{30}$$

The substitution of (25) and (30) into (29) and finally employing the Hopital's rule lead to the stress intensity factors for the embedded crack as follows:

$$k_{Li} = \frac{\mu}{2}\left((\alpha_i'(-1))^2 + (\gamma_i'(-1))^2\right)^{\frac{1}{4}} g_{zi}(-1)$$
$$k_{Ri} = -\frac{\mu}{2}\left((\alpha_i'(1))^2 + (\gamma_i'(1))^2\right)^{\frac{1}{4}} g_{zi}(1), i = 1, 2, \ldots, N_1 \tag{31}$$

Analogously, for an edge crack, the stress intensity factor reduces to

$$k_{ij} = \mu[(\alpha_j'(-1))^2 + (\gamma_j'(-1))^2]^{1/4} g_{zj}(-1)\, j = N_1 + 1, N_1 + 2, \ldots, N \tag{32}$$

Substituting (26) into (23) and (25) and discretizing the domain, $-1 \le p \le 1$, by $m + 1$ segments, the integral equations reduced to the following system of matrix equations:

$$\begin{bmatrix} H_{11} & H_{12} & \ldots & H_{1N} \\ H_{21} & H_{22} & \ldots & H_{2N} \\ \vdots & \vdots & \ddots & \vdots \\ H_{N1} & H_{N2} & \cdots & H_{NN} \end{bmatrix} \begin{bmatrix} g_{z1}(p_n) \\ g_{z2}(p_n) \\ \vdots \\ g_{zN}(p_n) \end{bmatrix} = \begin{bmatrix} q_1(s_r) \\ q_2(s_r) \\ \vdots \\ q_N(s_r) \end{bmatrix}, \tag{33}$$

where the collocation points are

$$s_r = \cos\left(\frac{\pi r}{m}\right) r = 1, 2, \ldots, m - 1,$$
$$p_n = \cos\left(\frac{\pi(2n-1)}{2m}\right) n = 1, 2, \ldots, m. \tag{34}$$

The components of matrix in (33) are

$$H_{ij} = \begin{bmatrix} A_{j1}k_{ij}(s_1, p_1) & \cdots & A_{jm-1}k_{ij}(s_1, p_{m-1}) & A_{jm}k_{ij}(s_1, p_m) \\ \vdots & \ddots & \vdots & \vdots \\ A_{j1}k_{ij}(s_{m-1}, p_1) & \cdots & A_{jm-1}k_{ij}(s_{m-1}, p_{m-1}) & A_{jm}k_{ij}(s_{m-1}, p_m) \\ A_{j1}B_{ij}(p_1) & \cdots & A_{jm-1}B_{ij}(p_{m-1}) & A_{jm}B_{ij}(p_m) \end{bmatrix}, \tag{35}$$

where δ_{ij} in the last row of designates the Kronecker delta, $\Delta_i(p_j) = \sqrt{[\alpha_i'(p)]^2 + [\gamma_i'(p)]^2}$. The components of vectors in (33) are

$$g_{zj}(p_n) = [g_{zj}(p_1)g_{zj}(p_2)\ldots g_{zj}(p_m)]^T$$
$$q_j = [\sigma_{nz_i}(x_j(s_1), y_j(s_1)) \quad \sigma_{nz_i}(x_j(s_2), y_j(s_2)) \quad \cdots \quad \sigma_{nz_i}(x_j(s_{m-1}), y_j(s_{m-1})) \quad 0]^T \quad j = 1, \ldots, N_1$$
$$q_j = [\sigma_{nz_i}(x_j(s_1), y_j(s_1)) \quad \sigma_{nz_i}(x_j(s_2), y_j(s_2)) \quad \cdots \quad \sigma_{nz_i}(x_j(s_{m-1}), y_j(s_{m-1})) \quad \sigma_{nz_i}(x_j(1), y_j(1))]^T$$
$$j = N_1 + 1, \ldots, N \tag{36}$$

In the above equalities, superscript T stands for the transpose of a vector and A_{jk} and $B_{ij}(p)$ are

$$A_{jk} = \frac{\pi}{m}\begin{cases} 1 & j = 1, \ldots, N_1 \\ 1 - P_k & j = N_1 + 1, \ldots, N, \; k = 1, 2, \ldots, m \end{cases},$$
$$B_{ij}(p) = \begin{cases} \delta_{ij}\sqrt{(\alpha_i'(p))^2 + (\gamma_i'(p))^2} & i = 1, \ldots, N_1 \\ k_{ij}(1, p) & i = N_1 + 1, \ldots, N \end{cases}. \tag{37}$$

6 Numerical and discussion

To verify the validity of the present work, let us consider the crack with length $2l$ which is under uniform shear impact tractionτ_0. The crack center is located on the x-axis of half-plane and is parallel to the boundary. By setting $h \to \infty$, in Eq. (24) and solving the relevant integral equations the non-dimensional dynamic stress intensity factor is obtained, which is identical with that given in Wei et al., 2000, Zhang et al., 2003. The analysis developed in preceding section, allows the consideration of a half-plane with multiple cracks subjected to shear traction. Two kinds of loading are chosen for the numerical calculations. The quantities of interest are the dimensionless stress intensity factors, $k(t)/k_0$. For convenience, the dynamic SIFs are normalized by $k_0 = \tau_0\sqrt{l}$ for constant traction and $k_0 = \tau_0/\sqrt{l}$ for the point load (Fig. 2).

Subsequently, let us consider a half-plane weakened by two embedded collinear cracks under anti-plane impact load, Fig. 3. In this example, interaction of two growing straight cracks with fixed centers subjected to the anti-plane impact load is considered. In this case, a considerable increase in $k(t)/k_0$ can be observed as l increases.

In the next example, we study the effect of the cracks orientation on dynamic stress intensity factors of crack tips Fig. 4. Crack L_1R_1 is fixed while L_2R_2 is rotating around its center, where θ is the angle between crack L_2R_2 and the x-axis. Note that, the variations of stress intensity factors of the tips L_1 and R_1 are not significant and are due to the change in the interaction between cracks. In a narrow band around$\theta = 3\pi/4$, the traction on the crack L_2R_2 vanishes; therefore, the stress intensity factors are very small.

Figure 5 shows the variation of dimensionless stress intensity factors, $k(t)/k_0$ of a stationary curved crack, and a growing straight crack with fixed center under point load. Fig. 5 indicates that the values of $k(t)/k_0$ of the two approaching crack tips are so large, whereas the opposite is true for crack tips L_1 and L_2. The parametric representations of straight and curved cracks are, respectively:

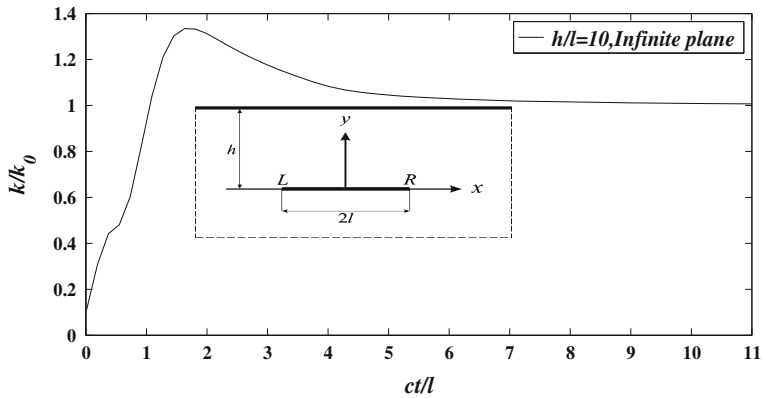

Fig. 2 Variation of the normalized dynamic stress intensity factor of one crack with cl/t

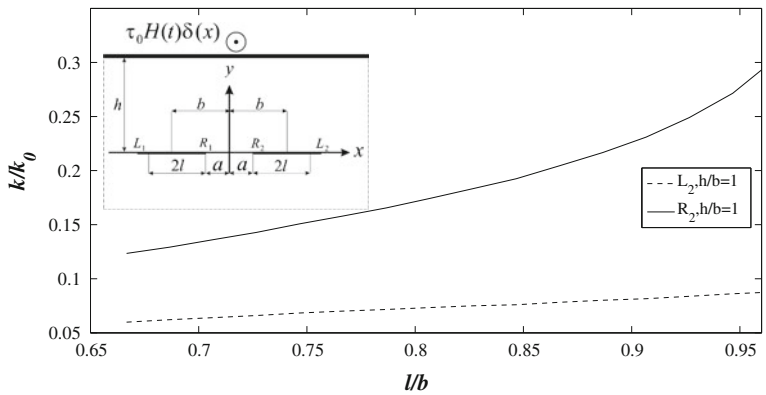

Fig. 3 Dynamic stress intensity factors of two collinear cracks with l/b

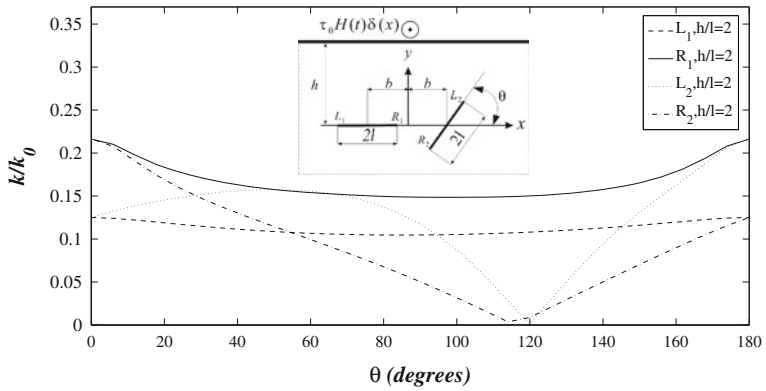

Fig. 4 Dynamic stress intensity factors of a fixed and rotating cracks under anti-plane point loading

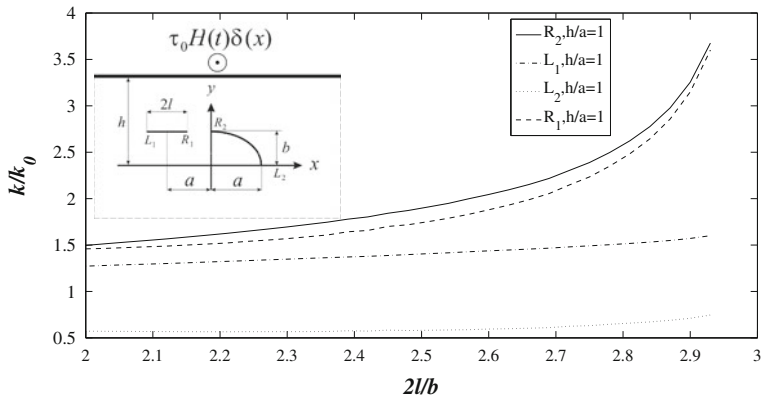

Fig. 5 Dynamic stress intensity factors of a curved crack and a straight crack subjected to anti-plane point loading

$$
\begin{aligned}
&\alpha_1(q) = -a + lq,\\
&\beta_1(q) = b,\\
&\alpha_2(q) = a\cos\left[\frac{\pi}{4}(1-q)\right],\\
&\beta_2(q) = a\cos\left[\frac{\pi}{4}(1-q)\right]. \qquad -1 \le q \le 1
\end{aligned}
$$

Subsequently, let us consider the two curved crack problem in a half-plane when the cracks are subjected to the impact surface tractions. These two curved cracks are portions of the perimeter of an ellipse with parametric equations

$$
\begin{aligned}
&\alpha_i(q) = (-1)^i a\cos\left[1/2(1-(-1)^i q)tg^{-1}\left(\frac{a}{b}\cot g\phi\right)\right],\\
&\beta_i(q) = (-1)^i b\sin\left[1/2(1-(-1)^i q)tg^{-1}\left(\frac{a}{b}\cot g\phi\right)\right]. \qquad -1 \le q \le 1, i = 1, 2,
\end{aligned}
$$

The length of major and minor semi-axes of the ellipse is a and b, respectively. The problem is symmetric with respect to the y-axis. As it can be seen that the stress intensity factors at cracks tips R_1 and R_2 are larger than those for tips L_1 and L_2. The dimensionless stress intensity factor of crack tip is decreased by a decrease in the crack length (Fig. 6).

In the next examples, we consider two cracks, one edge crack with length $2l_2 = h/2$ and a rotating embedded crack with length $2l_1 = h$. The half-plane is under point load traction on the boundary. The non-dimensionalized stress intensity factors verses angle θ are depicted in Figs. 7 and 8. In addition, the range of variation of SIF at crack tip L_2 is not significant. From Figs. 7 and 8, we may conclude that the SIF of edge crack is mainly caused by the geometric asymmetry of the crack rather than its interaction with the embedded crack.

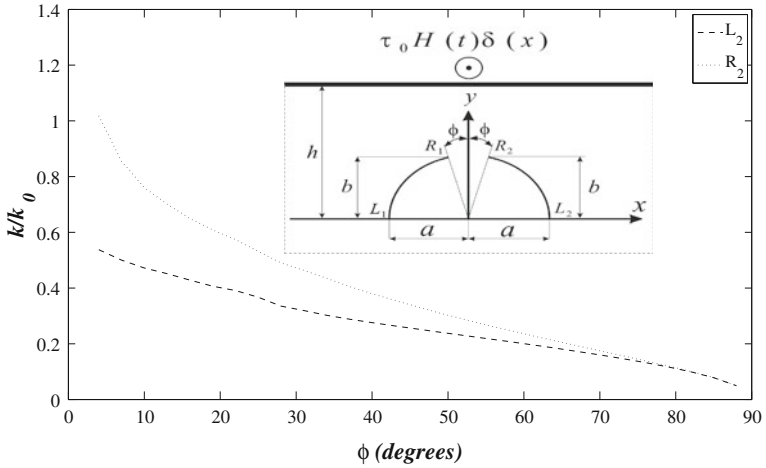

Fig. 6 Variations of the normalized stress intensity factor of two curved cracks

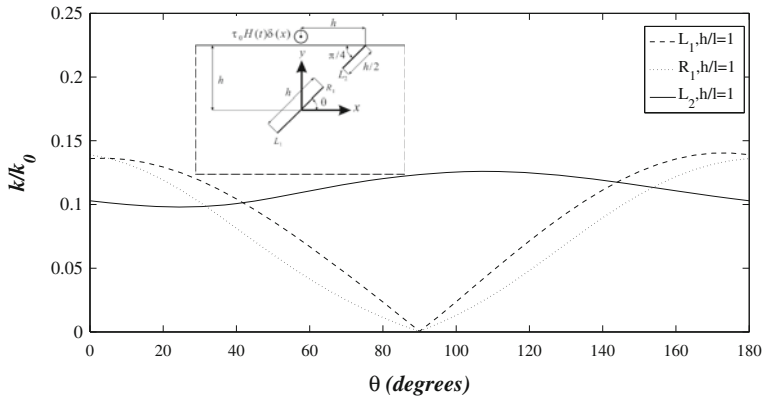

Fig. 7 Dynamic stress intensity factor for an edge and rotating embedded crack

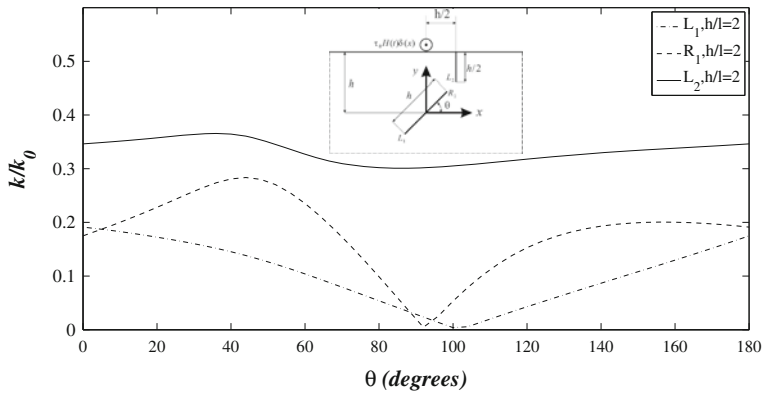

Fig. 8 Dynamic stress intensity factor for an edge and rotating crack under anti-plane point loading

As the last example, the interaction between a curved edge crack and a embedded crack situated on the x-axis is studied. The edge crack is a quarter of the perimeter of an ellipse with the lengths of major and minor semi-axes a and b, respectively. The dynamic stress intensity factors of the edge crack are larger than that of the embedded crack but exhibit smaller variations (Fig. 9).

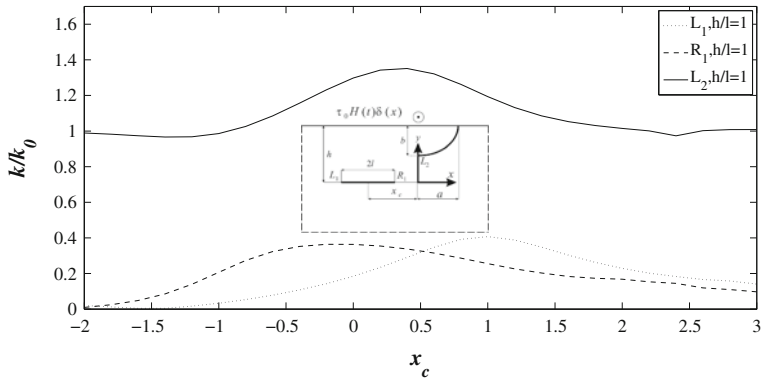

Fig. 9 Dynamic stress intensity factor for a curved edge and an embedded crack

7 Conclusions

Half-plane containing multiple curved cracks is analyzed under action of the sudden anti-plane shear impact loads. Using the one-sided and two-sided Laplace transform methods, the associated boundary value problem is reduced to solving singular integral equations for the Volterra dislocation density. Validation of the presented method was carried out by considering a single crack in an infinite plane under impact load. The presented examples of the embedded and edge cracks revealed that:

(1) The dynamic stress intensity factor (DSIF) of the crack tip increases as it approaches the point load. Conversely, DSIF decreases at a crack tip as it approaches the boundary of the half-plane.
(2) Dynamic stress intensity factor at crack tips increased by an increase in the crack length.
(3) The interaction between multiple embedded and edge cracks in various examples is studied.
(4) The results are in excellent agreement with the analytical solutions obtained in Zhang et al. [13].

Appendix

We utilize the polar coordinates $x = r\cos\theta,\ \ y = r\sin\theta$. The real variable $S_L \le t < \infty$ is defined as

$$t = -\eta r\cos\theta + r\sin\theta\sqrt{S_L^2 - \eta^2} \tag{38}$$

The solution of Eq. (14) for η is

$$\eta_{\pm}(r,\theta,t) = -\frac{t}{r}\cos\theta \pm i\left(\frac{t^2}{r^2} - S_L^2\right)^{\frac{1}{2}}\sin\theta \tag{39}$$

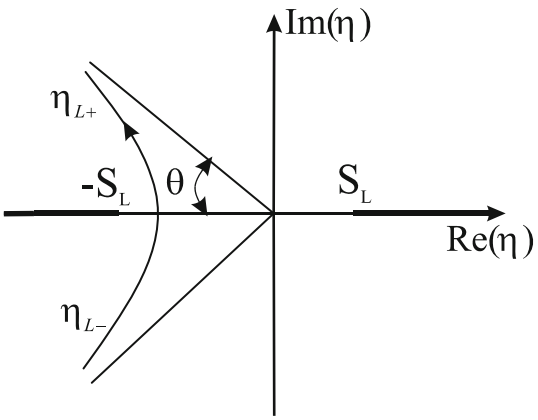

Fig. 10 Path of integration in the η-plane

In the complex η-plane, the hyperbola (39) intersects the real axis at $\eta = -S_L \cos\theta$ which is not on the branch cuts. The desired path of integration in the η-plane for Eq. (13) is defined by the Eq. (39), Fig 10. Furthermore, the path does not cross the branch cuts, and Eq. (13) becomes:

$$\bar{w}(x, y, s) = \frac{-ib_z}{4\pi s}\left[\int_{\infty}^{S_L r} \frac{1}{\eta_-}\frac{\partial \eta_-}{\partial t} e^{-st}\mathrm{d}t + \int_{S_L r}^{\infty} \frac{1}{\eta_+}\frac{\partial \eta_+}{\partial t} e^{-st}\mathrm{d}t\right]. \tag{40}$$

The integrals in Eq. (40) may be simplified by employing the procedure described in Achenbach.

References

1. Maue, A.W.: Die beuguhg elastischer wellen an der halbebene. ZAMM **33**, 1–10 (1953)
2. Loeber, J.F., Sih, G.C.: Diffraction of anti-plane shear waves by a finite crack. Acoust. Soc. Am. **44**, 90–98 (1968)
3. Thau, S.A., Hwei, L.T.: Transient stress intensity factor for a finite crack in an elastic solid caused by a dilatational wave. Int. J. Solids Struct. **7**, 731–750 (1971)
4. Sih, G.C., Embley, G.T.: Sudden twisting of a penny-shaped crack. ASME. Appl. Mech. **39**, 395–400 (1972)
5. Kuo, A.Y.: Transient intensity factors of an interfacial crack between, two dissimilar anisotropic half-spaces. Appl. Mech. **51**, 7176 (1984)
6. Ang, W.T.: A crack in an anisotropic layered material under the action of impact loading. Appl. Mech. **55**, 120–125 (1988)
7. Babaei, R., Lukasiewicz, S.A.: Dynamic response of a crack functionally graded material between two dissimilar half-planes under anti-plane shear impact load. Eng. Fract. Mech. **60**, 479–487 (1998)
8. Wang, B.L., Han, J.C., Du, S.Y.: Multiple crack problem in nonhomogeneous composite materials subjected to dynamic anti-plane shearing. Int. J. Fract. **100**, 343–353 (1999)
9. Chen, Z.T., Karihaloo, B.L.: Dynamic response of a cracked piezoelectric ceramic arbitrary electro-mechanical impact. Int. J. Solids Struct. **36**, 5125–5133 (1999)
10. Zhang, Ch.: Transient elastodynamic anti-plane crack analysis of anisotropic solids. Int. J. Fract. **37**, 6107–6130 (2000)
11. Wei, P.J., Zhang, S.Y., Wu, Y.L., Li, K.Y.: Dynamic SIF of interface crack problem between two dissimilar viscoelastic bodies under impact loading. Int. J. Fract. **105**, 127–136 (2000)
12. Zhao, X., Meguid, S.A., Liew, K.M.: The transient response of bonded piezoelectric and elastic half-space with multiple interfacial collinear cracks. Acta. Mech. **159**, 11–27 (2002)
13. Zhang, Ch., Sladek, J., Sladek, V.: Effects of material gradients on transient dynamic mode-III stress intensity factors in a FGM. Int. J. Solids Struct. **40**, 5251–5270 (2003)
14. Zhao, X.: The stress intensity factor history for an advancing crack in a transversely isotropic solid under 3-D loading. Int. J. Solids Struct. **40**, 89–103 (2003)
15. Feng, W.J., Zou, Z.Z.: Dynamic stress field for torsional impact of the penny-shaped crack in a transversely isotropic functionally graded strip. Int. J. Eng. Sci. **41**, 1729–1739 (2003)
16. Sladek, J., Sladek, V., Zhang, C.Z.: Dynamic response of a crack in a functionally graded material under an anti-plane shear impact load. Eng. Mater. **251**(252), 123–129 (2003)
17. Wang, B.L., Mai, Y.W.: A periodic array of cracks in functionally graded materials subjected to transient loading. Int. J. Eng. Sci. **44**, 351–364 (2006)
18. Itou, S.: Transient dynamic stress intensity factors around two rectangular cracks in a nonhomogeneous interfacial layer between two dissimilar elastic half-spaces under impact load. Acta. Mech. **192**, 89–110 (2007)
19. Wu, K.C., Chen, J.C.: Transient analysis of collinear cracks under anti-plane dynamic loading. Eng. Proc. **10**, 924–929 (2011)
20. Monfared, M.M., Ayatollahi, M.: Elastodynamic analysis of a cracked orthotropic half-plane. Appl. Math. Model. **36**, 2350–2359 (2012)
21. Weertman, J.: Dislocation Based Fracture Mechanics. World Scientific, Singapore (1996)
22. Achenbach, J.D.: Wave Propagation in Elastic Solids. North-Holland, Amsterdam (1976)
23. Erdogan, F., Gupta, G.D., Cook, T.S.: Numerical solution of singular integral equations. In: Sih, G.C. (ed.) Method of Analysis and Solution of Crack Problems. Noordhoof, Leyden
24. Liebowitz, H.: Fracture Mechanics. Academic Press, New York (1968)